Hydrol. Earth Syst. Sci., 19, 3829–3844, 2015
www.hydrol-earth-syst-sci.net/19/3829/2015/
doi:10.5194/hess-19-3829-2015

Hydrology and Earth System Sciences
Open Access

GlobWat – a global water balance model to assess water use in irrigated agriculture

J. Hoogeveen[1,3], **J.-M. Faurès**[1], **L. Peiser**[1], **J. Burke**[2], **and N. van de Giesen**[3]

[1]Food and Agriculture Organization of the United Nations, Rome, Italy
[2]World Bank, Washington, D.C., USA
[3]Delft University of Technology, Delft, the Netherlands

Correspondence to: J. Hoogeveen (jippe.hoogeveen@fao.org)

Received: 1 December 2014 – Published in Hydrol. Earth Syst. Sci. Discuss.: 20 January 2015
Accepted: 9 August 2015 – Published: 10 September 2015

Abstract. GlobWat is a freely distributed, global soil water balance model that is used by the Food and Agriculture Organization (FAO) to assess water use in irrigated agriculture, the main factor behind scarcity of freshwater in an increasing number of regions. The model is based on spatially distributed high-resolution data sets that are consistent at global level and calibrated against values for internal renewable water resources, as published in AQUASTAT, the FAO's global information system on water and agriculture. Validation of the model is done against mean annual river basin outflows.

The water balance is calculated in two steps: first a "vertical" water balance is calculated that includes evaporation from in situ rainfall ("green" water) and incremental evaporation from irrigated crops. In a second stage, a "horizontal" water balance is calculated to determine discharges from river (sub-)basins, taking into account incremental evaporation from irrigation, open water and wetlands ("blue" water). The paper describes the methodology, input and output data, calibration and validation of the model. The model results are finally compared with other global water balance models to assess levels of accuracy and validity.

1 Introduction

Modelling of the world's hydrological cycle is important to assess, among others, water resources availability and the sustainability of their use, the impact of climate change, and the influence on global food production (Wood et al., 2011). With regard to global food production, one of the major questions on the future of irrigated agriculture is whether there will be sufficient freshwater to satisfy the growing needs of agricultural and non-agricultural users. Agriculture accounts for about 70 % of the freshwater withdrawals in the world (FAO, 2013), while consumptive use of water in agriculture (water that is evaporated on irrigated fields) accounts for about 90 % of all of the water that is evaporated as a result of human intervention. Irrigated agriculture is therefore the main component of water demand and a driver of scarcity of freshwater in an increasing number of regions.

AQUASTAT (FAO, 2013), the Food and Agriculture Organization's (FAO's) information system on water and agriculture, collects its information mainly from country statistics and grey literature. As part of the AQUASTAT programme, FAO distributes and contributes to the maintenance and development of the Global Map of Irrigation Areas (Siebert et al., 2007, 2010, 2013), which is compatible with AQUASTAT country figures for areas equipped for irrigation. Assessing the impact of irrigation on water scarcity requires information about the geographical distribution of water use

in irrigation. The Global Map of Irrigation Areas provides information about the distribution of land under irrigation, but data collection through AQUASTAT country surveys has shown that country statistics for agricultural water withdrawals are not always available, and when they exist, they are often unreliable. In most cases they are rough estimates based on water use per unit area of land equipped for irrigation.

Actual water use in annual water balances is changing over time as cropping patterns and cropping intensities shift and change, sometimes in response to available water resources. Therefore a consistent global picture of water withdrawals and consumptive use in irrigated agriculture cannot be obtained without some reference to modelled estimates. Simulation of water use in irrigated agriculture at global scale at the highest available resolution would therefore address a gap in hydrological understanding under contemporary land and water use patterns.

A number of global models exist that simulate water use in agriculture. WaterGAP (Döll and Fiedler, 2008; Hunger and Döll, 2008; Alcamo et al., 2007), WBMplus (Wisser et al., 2010), GEPIC (Liu, 2009; Liu and Yang, 2010), LPJmL (Biemans, 2012; Rost et al., 2008) and PCR-GLOBWB (Wada et al., 2014) are all global hydrological models that have been used to calculate water use by irrigated agriculture. Most of these models are sophisticated hydrological models that are used for detailed water balance analyses in which consumptive water use in agriculture is only one of the components of the water balance rather than the main focus of analysis. Almost all of them are developed at a spatial disaggregation (30 arcmin or coarser) which is not directly comparable with the heterogeneity and spatial variability of irrigation as captured in the FAO's high-resolution (5 arcmin) Global Map of Irrigation Areas or in other global agriculture land use data such as that available through FAO and IIASA's Global Agro-Ecological Zones portal (FAO/IIASA, 2012).

To overcome this incompatibility between global hydrological models and the Global Map of Irrigation Areas, Siebert and Döll (2008, 2010) developed the Global Crop Water Model (GCWM) to calculate irrigated crop water requirements on a grid resolution of 5 arcmin by using the MIRCA2000 data set (Portmann et al., 2008). However, contrary to the earlier mentioned models, the GCWM does not simulate the influence of incremental crop evapotranspiration on the hydrological cycle to the extent that model results can be calibrated or validated on river discharges.

Therefore, in order to be able to estimate current and future water use in agriculture objectively and the consequent impact on river basin mean annual flow, a global water balance model, GlobWat, was developed. The defining feature of the model is that it is based on a set of spatially differentiated data sets at 5 arcmin resolution that are consistent at global level, and that model outputs are validated against actual basin outflows.

The model is designed to complement other FAO data sets and models as used for AQUASTAT (FAO, 2013), Global Agro-Ecological Zones (FAO/IIASA, 2012) and Global Perspective Studies (FAO, 2006, 2011a).

2 Methodology

Precipitation provides part of the water crops' need to satisfy their transpiration requirements. The soil stores part of the precipitation water, which is later evaporated or transpired by plants. In humid climates, the water stored by the soil is sufficient to ensure satisfactory growth in rainfed agriculture. Instead, in climates with extended dry periods, irrigation is necessary to compensate for the evaporation deficit due to insufficient precipitation. The purpose of the modelling exercise is to estimate net irrigation water requirements on irrigated land. In terms of a hydrological balance, this is incremental evaporation due to the import of water onto land. Net irrigation water requirements in irrigation are calculated as the volume of water needed to compensate for the deficit between potential crop evaporation and effective precipitation over the growing period of the crop. This requirement varies considerably with climatic conditions, seasons, crops and soil types. Following Savenije (2004), the model description uses the term evaporation (E) to describe evaporative processes originating from soil evaporation, transpiration and interception. In agro-hydrology these processes are often referred to as evapotranspiration (ET).

GlobWat has spatially distributed input and output layers consisting of monthly precipitation, number of wet days per month, coefficient of variation of precipitation, monthly reference evaporation, maximum soil moisture storage capacity, maximum groundwater recharge flux, irrigated areas, land use, and areas of open water and wetlands. All these input layers are based on freely available spatial data sets with a resolution of 10 arcmin for the climate data sets and 5 arcmin for all the terrain and land data sets (details and references of the data sets are given in Table 3).

The global water balance is calculated in two steps. First a one-dimensional "vertical" water balance is solved (in daily time steps, on a spatial grid layer with a resolution of 5 arcmin) to calculate rainfed evaporation (including rainfed evaporation over open water and wetlands) and evaporation from irrigated areas. In a second step, a "horizontal" water balance for surface water is calculated (in monthly time steps, on the basis of a spatial layer with catchments) to correct for the incremental evaporation from open water and wetlands and to calculate river discharges from (sub-)basins taking into consideration the net water demand for irrigation. The monthly time step for the horizontal balance is justified, on the basis of the hydrological lag between daily rainfall events and outflows generated from runoff and effluent groundwater discharge, in combination with the size of the river basins considered. The use of vertical and horizon-

tal water balances helps to clarify discussions on "green" and "blue" water (Falkenmark and Rockström, 2004), as well as on water footprints (Hoekstra and Chapagain, 2007), since it can distinguish between evaporation attributable to land management (evaporation from in situ rainfall) and evaporation attributable to water management (evaporation resulting from the lateral import of water). The significance of open water and wetlands as evaporative "sinks" is also made explicit. A schematic representation of these two calculation steps is given in Fig. 1.

Under long-term, stationary conditions (therefore ignoring changes in hydrological storage), the model is based on two simple equations. For the vertical water balance,

$$P + E_{\text{incr-irr}} = E_{\text{rain}} + E_{\text{incr-irr}} + R_{\text{O}} + R, \quad (1)$$

and for the horizontal (surface) water balance,

$$Q_{\text{out}} = Q_{\text{in}} + R_{\text{O}} + R - E_{\text{incr-irr}} - E_{\text{incr-OW}} - E_{\text{incr-wetl}}, \quad (2)$$

where P is precipitation ($\text{L}^3\,\text{T}^{-1}$), E_{rain} is rainfed evaporation ($\text{L}^3\,\text{T}^{-1}$), Q_{in} is inflow ($\text{L}^3\,\text{T}^{-1}$), R_{O} is (sub-)surface runoff ($\text{L}^3\,\text{T}^{-1}$), R is groundwater recharge (in step 1)/baseflow (in step 2) ($\text{L}^3\,\text{T}^{-1}$), $E_{\text{incr-irr}}$ is incremental evaporation from irrigation ($\text{L}^3\,\text{T}^{-1}$), $E_{\text{incr-OW}}$ is incremental evaporation over open water ($\text{L}^3\,\text{T}^{-1}$), $E_{\text{incr-wetl}}$ is incremental evaporation over wetlands ($\text{L}^3\,\text{T}^{-1}$) and Q_{out} is outflow ($\text{L}^3\,\text{T}^{-12}$), where L is length and T is time.

The detailed calculations procedure for the respective model components is explained below.

3 Soil water balance

The soil water balance model is similar to the Thornwaite and Mather procedure (Steenhuis and Van der Moolen, 1986) adapted for daily time steps. The basic soil water balance equation for this model is as follows:

$$P = E_{\text{rain}} + R + R_{\text{O}} + \Delta S/\Delta t, \quad (3)$$

with P = precipitation (mm day^{-1}), E_{rain} = rainfall-dependent evaporation (mm day^{-1}), R = groundwater recharge (mm day^{-1}), R_{O} = (sub-)surface runoff (mm day^{-1}), ΔS = changes in soil moisture storage (mm) and Δt = time step (day).

The computation of water balance is carried out on a spatial resolution of 5 arcmin grid cells and in daily time steps taking account of spatial variations in rainfall, evaporative power of the atmosphere and soil properties.

4 Precipitation

Daily precipitation is generated from monthly figures by using a mixed Bernoulli gamma distribution function (Wilks and Wilby, 1999). First the number of wet days is randomly distributed over the month by using a Bernoulli distribution, and then the amount of monthly precipitation is randomly distributed over the wet days by using a gamma distribution with parameters derived from the data set with coefficients of variation of precipitation.

Usually, precipitation generators use Markov chains to generate precipitation events (Schoof and Pryor, 2008). However, the data sets used do not include information to parameterise these Markov chains. To take into consideration that the chance of rainfall after a wet day is higher than the chance of rainfall after a dry day, the following simple adjustment was made:

$$P_{\text{wet wet}} = (1 + \text{corr}) \times P_{\text{wet mean}} \quad (4)$$

and

$$P_{\text{wet dry}} = P_{\text{wet mean}} \times (1 - P_{\text{wet wet}}) / (1 - P_{\text{wet mean}}), \quad (5)$$

with $P_{\text{wet wet}}$ is the probability of a wet day after a wet day, $P_{\text{wet dry}}$ is the probability of a wet day after a dry day, and $P_{\text{wet mean}}$ is the average probability of a wet day calculated as

$$P_{\text{wet mean}} = \text{wet days/days of the month}. \quad (6)$$

corr = correction coefficient is calculated as

$$\text{corr} = 0.5 \times (\text{days of the month} - \text{wet days})/\text{days of the month}. \quad (7)$$

Applying this adjustment, the chance of a wet day after a wet day is almost 1.5 times as high when the number of wet days approaches 0, while the chance of a wet day after a wet day approaches the average chance of a wet day if the number of wet days is high.

The spatial distribution of all climate data is determined by the CRU CL 2.0 data set (New et al., 2002). This data set has been chosen to obtain maximum consistency between precipitation and reference evaporation, and because it describes average climatic conditions, which are comparable to the data available in AQUASTAT.

5 Rainfall-dependent evaporation

Rainfall-dependent evaporation (E_{rain}) is assumed to be equal to the maximum evaporation of a land use or vegetation type when evaporation is not hampered by water shortage. Maximum evaporation is calculated by multiplying reference evaporation by a crop or land use factor (Allen et al., 1998). In dry periods, when the available soil moisture is reduced below a certain level, lack of water reduces evaporation to an extent proportional to the available soil moisture.

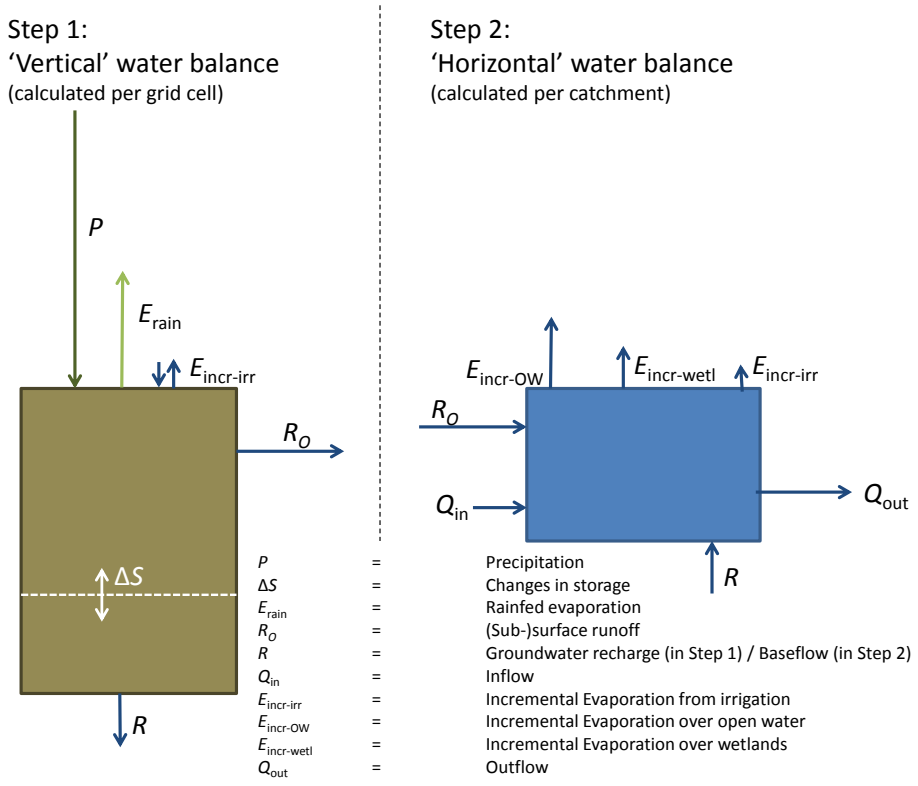

Figure 1. Schematic representation of modelling steps.

Table 1. Vegetation types derived from FAO's Global Agricultural Systems Map.

Vegetation class	*Kc* factor
Rainfed agriculture: dry tropics	0.9
Rainfed agriculture: humid tropics	1
Rainfed agriculture: highlands	0.9
Rainfed agriculture: subtropics	1
Rainfed agriculture: temperate	1
Rangelands: subtropics	0.8
Rangelands: temperate	0.9
Rangelands: boreal	0.8
Forest	1.1
Desert	0.7
Other	1

In equations:

$$E_{\text{rain}}(t) = K_{\text{c}} \times E_{\text{o}}(t) \text{ for } S_{\text{max}} \geq S(t-1) \geq S_{\text{eav}} \quad (8)$$

$$E_{\text{rain}}(t) = K_{\text{c}} \times E_{\text{o}}(t) \times S(t-1)/(S_{\text{eav}}) \text{ for } S(t-1) < S_{\text{eav}} \quad (9)$$

$$S_{\text{eav}} = 0.5 \times S_{\text{max}} \quad (10)$$

$$S_{\text{max}} = \text{Rt}_{\text{d}} \times \text{SC}_{\text{max}} \quad (11)$$

with t the time step indicator, $E_{\text{rain}}(t)$ the rainfed evaporation on t (mm day^{-1}), $E_{\text{o}}(t)$ the reference evaporation on t (mm day^{-1}), K_{c} the crop or land use factor (–), $S(t-1)$ the available soil moisture on $t-1$ (mm), S_{max} the maximum soil moisture storage (mm), S_{eav} the easily available soil moisture (mm), Rt_{d} the effective root depth (m), and SC_{max} the maximum soil moisture storage capacity (mm m^{-1}).

The crop or land use factor K_{c} is not constant over the year. It varies during the growing season, depending on the growing stage. However, for rainfed conditions, differentiated K_{c} factors were not applied, since no distinction was made between the different crops and their cropping calendars. The K_{c} factors used were attributed to the Global Agricultural Systems Map (FAO, 2011b) according to Table 1.

As can be seen from the equations above, the easily available soil moisture (S_{eav}) is defined as half the maximum soil moisture storage (S_{max}). In reality, easily available moisture depends on the type of plant, its growing stage and its soil type, and it varies from about 40 to 60 % of the maximum soil moisture storage capacity (SC_{max}) (Raes et al., 2012). For a global model, 50 % can be considered a reasonable approximation.

The spatial distribution of the maximum soil moisture storage capacity (SC_{max}) was derived from the Harmonised World Soil Database (FAO, 2012).

The effective root depth of vegetation is the part of the root zone from which the plant extracts the majority of the water it needs, and therefore it depends both on soil and plant characteristics as well as the amount of water available. There

are different ways to estimate the effective root depth, i.e. half the maximum root depth (Evans et al., 1996) or the soil depth in which 90 % of the weight of the roots is found (Allen et al., 1998; FAO, 1978). However, for a global model, such information is not available and therefore an initial effective rooting depth of 60 cm is assumed. Since the results of model computation are very sensitive to effective rooting depth and to soil moisture storage capacity (SC_{max}), both parameters were used to calibrate the model.

6 Groundwater recharge, actual available soil moisture and (sub-)surface runoff

Groundwater recharge is assumed to occur only above a threshold level when there is enough water available in the soil to percolate downward in the model. The recharge rate depends on a maximum possible groundwater recharge flux, which is derived from the Groundwater Resources of the World Map provided by the World-wide Hydrogeological Mapping and Assessment Programme (WHYMAP) (BGR and UNESCO, 2008), and is assumed to be proportional to the available soil moisture. The recharge component is assumed to contribute to the shallow groundwater circulation that appears as effluent seepage in the annually renewable water resource account of the respective basins. Given that all groundwater heads are generated by tectonic uplift and fluvial erosion, all groundwater flows in the model are assumed to enter the annual river basin balance and not enter permanent groundwater storage.

In equations:

$$R(t) = R_{max} \times (S(t-1) - S_{eav}) / (S_{max} - S_{eav}) \quad \text{for } S_{max} \geq S(t-1) \geq S_{eav}, \tag{12}$$

$$R(t) = 0 \text{ for } S(t-1) < S_{eav}, \tag{13}$$

with $R(t)$ the recharge flux on t (mm day^{-1}) and R_{max} the maximum groundwater recharge flux (mm day^{-1}).

The available soil moisture is calculated per day by adding ingoing and outgoing fluxes to the available soil moisture of the day before. Runoff occurs when the balance of the ingoing and outgoing fluxes exceeds the maximum soil moisture storage capacity.

In equations:

$$B(t) = S(t-1) + (P(t) - E_{rain}(t) - R_O(t)) \cdot \Delta t \tag{14}$$

If $B(t) < S_{max}$, then

$$S(t) = B(t), \tag{15}$$

$$R_O(t) = 0. \tag{16}$$

If $B(t) \geq S_{max}$, then

$$S(t) = S_{max}, \tag{17}$$

$$R_O(t) = (B(t) - S_{max}) / \Delta t, \tag{18}$$

with $B(t)$ the balance on t (mm), $R_O(t)$ the (sub-)surface runoff on t (mm day^{-1}) and $S(t)$ the available soil moisture on t (mm).

7 Evaporation for crops under irrigation

Evaporation for crops under irrigation is calculated by multiplying reference evaporation by a crop and growing stage specific factor according to the FAO Penman–Monteith method (Allen et al., 1998). It is assumed that there is always enough water available to ensure that crops under irrigation never suffer water stress.

The evaporation of a crop under irrigation (E_c) is calculated as follows:

$$E_c(t) = K_c \times E_o(t), \tag{19}$$

with $E_c(t)$ crop evaporation under irrigation on t (mm day^{-1}), $E_o(t)$ reference evaporation on t (mm day^{-1}) and K_c the rop or land use factor (–).

Crop coefficients (K_c) have been derived for four different growing stages: the initial phase (just after sowing), the development phase, the mid-phase and the late phase (when the crop is ripening to be harvested). In general, these coefficients are low during the initial phase, after which they increase during the development phase to high values in the mid-phase, and again decrease in the late phase. It is assumed that the initial phase, the development phase and the late phase each take 1 month for each crop, while the duration of the mid-phase varies according to the type of crop. For example, the growing season for wheat in Morocco starts in October and ends in April, as follows: initial phase: October ($K_c = 0.4$); development phase: November ($K_c = 0.8$); mid-phase: December–March ($K_c = 1.15$); and late phase: April ($K_c = 0.3$).

Evaporation requirements of crops in irrigated agriculture are calculated by converting data of irrigated area by crop (at the national level) into a cropping calendar with monthly occupation rates of the land equipped for irrigation. Cropping calendars have been developed by AQUASTAT (http://www.fao.org/nr/water/aquastat/water_useagr/index2.stm) for each of the countries or country groups of the study (except for China, India and the United States, which were divided into several zones of homogenous cropping patterns). Table 2 presents the irrigation cropping calendar for Morocco, derived from AQUASTAT data for the year 2004.

The rate of evaporation coming from the irrigated area per month and per grid cell is calculated by multiplying the area equipped for irrigation as derived from the Global Map of Irrigation Areas (Siebert et al., 2007) by cropping intensity and crop evaporation for each crop:

$$E_{\text{c-total}}(t) = I_{\text{A}} \times \Sigma_{\text{c}} \left(C_{\text{Ic}} \times E_{\text{c}}(t) \right), \quad (20)$$

with $E_{\text{c-total}}(t)$ total evaporation for all crops under irrigation on t in mm day^{-1}, I_{A} the area equipped for irrigation as percentage of cell area for the given grid cell, c crop under irrigation, Σ_{c} the sum over the different crops, C_{Ic} the cropping intensity for crop c and $E_{\text{c}}(t)$ the crop evaporation on t in mm day^{-1}, varying for each crop and each growth stage.

The difference between the calculated evaporation of the irrigated area, E_{c}, and the evaporation provided by rainfall, E_{rain}, is equal to the incremental evaporation due to irrigation, which equals the net irrigation water requirement:

$$E_{\text{incr-irr}}(t) = E_{\text{c-total}}(t) - E_{\text{rain}}(t), \quad (21)$$

with $E_{\text{incr-irr}}(t)$ the incremental evaporation due to irrigation on t (mm day^{-1}).

8 Evaporation from open water and swamps

A special correction is applied for grid cells existing of open water or swamps. In these areas, the actual evaporation depends on heat storage in lakes and reservoirs, which is related to the depth of the water bodies, and, in the case of swamps and wetlands, the vegetation. In the model, evaporation from open water is computed in a simplified manner as follows:

$$E_{\text{ow}}(t) = K_{\text{ow}} \times E_{\text{o}}(t) \quad (22)$$

and

$$B(t) = (P(t) - E_{\text{ow}}(t)) \cdot \Delta t, \quad (23)$$

with $E_{\text{ow}}(t)$ actual evaporation over open water on t (mm day^{-1}), K_{ow} the open water coefficient (–) and $B(t)$ the open water balance on t (mm).

If $B(t) < 0$, then

$$R_{\text{O}}(t) = 0, \quad (24)$$
$$E_{\text{rain}}(t) = P(t), \quad (25)$$
$$E_{\text{incr-ow}}(t) = (-1 \times B(t))/\Delta t. \quad (26)$$

If $B(t) \geq 0$, then

$$R_{\text{O}}(t) = B(t)/\Delta t, \quad (27)$$
$$E_{\text{rain}}(t) = E_{\text{ow}}(t)/\Delta t, \quad (28)$$
$$E_{\text{incr-ow}}(t) = 0, \quad (29)$$

with $E_{\text{incr-ow}}(t)$ the incremental evaporation over open water on t (mm day^{-1}).

Evaporation over swamps and wetlands is calculated separately, but in the same way as evaporation over open water. For this study, open water evaporation and evaporation over swamps and wetlands is assumed to be 10 % higher than reference evaporation ($K_{\text{ow}} = 1.1$).

The spatial distribution of open water and wetlands was derived from the global map of lakes and wetlands (Lehner and Döll, 2004).

It was decided to make a distinction between the rainfall-dependent evaporation over open water and incremental evaporation over open water, to make it possible to distinguish between evaporation of water that is available from the "vertical" water balance (the rainfall minus evaporation) and the water that has to come from outside the spatial domain of calculation (the incremental evaporation).

9 River basin discharges

To calculate discharges from river basins and sub-basins, a global map of river basins was used which was developed in the framework of the FAO's study "The state of the world's land and water resources for food and agriculture – managing systems at risk" (FAO, 2011b). For this study, major river basins and their sub-basins were delineated from the HydroSHEDS database. Sub-basins were named and assigned a flow direction, indicating the sub-basin directly downstream of each sub-basin. Aggregated water balances were calculated on a monthly time step by subtracting all evaporation occurring over the sub-basin from the sum of the total precipitation over the sub-basin and the inflow from upstream basins (Eq. 30).

$$B_{\text{sb}}(t) = Q_{\text{in}}(t) + \sum P(t) - \sum E(t) \quad (30)$$

with B_{sb} the water balance of aggregated grid cells in a sub-basin (m^3 month^{-1}), t the time step indicator, Q_{in} the incoming flow in the sub-basin calculated as the sum of the outflow from all upstream sub-basins (m^3 month^{-1}), $\sum P$ the precipitation summed over all grid cells in the sub-basin (m^3 month^{-1}) and $\sum E$ the total evaporation summed over all grid cells in the sub-basin (m^3 month^{-1}).

There is a lag between the time water enters a sub-basin and the time it gets out, and some of the inflow is trapped in storage in the sub-basin. To take the time lag and storage effect into account, a simple linear reservoir model (De Zeeuw, 1973) is used to calculate monthly values for river discharges and the amount of water stored per sub-basin:

$$S_{\text{sb}}(t) = S_{\text{sb}}(t-1) + (B_{\text{sb}}(t) - Q_{\text{out}}(t-1)) \cdot \Delta t \quad (31)$$

and

$$Q_{\text{out}}(t) = S_{\text{sb}}(t) \times F \quad (32)$$

with S_{sb} the river sub-basin storage (m^3), Δt the time step (month), Q_{out} the outflow from the sub-basin (m^3 month^{-1}) and F the response factor (1/month).

The response factor F in Eq. (32) depends on the size and the characteristics of the sub-basin. It can be defined as the one over the retention time of the water in the basin in months. For small, quickly reacting sub-basins, the monthly

Table 2. Cropping calendar in irrigation for Morocco for the year 2004.

Crop under irrigation	Irrigated area (1000 ha)		Crop area as share (per cent) of the total area actually irrigated by month											
			J	F	M	A	M	J	J	A	S	O	N	D
Wheat	355		24 %	24 %	24 %	24 %						24 %	24 %	24 %
Rice	8				1 %	1 %	1 %	1 %	1 %					
Maize	60					4 %	4 %	4 %	4 %	4 %				
Barley	95		6 %	6 %	6 %							6 %	6 %	6 %
Potatoes	31													
– First season		20	1 %	1 %	1 %	1 %								1 %
– Second season		10					1 %	1 %	1 %	1 %	1 %			
Sugar beet	75				5 %	5 %	5 %	5 %	5 %	5 %				
Sugar cane	23		2 %	2 %	2 %	2 %	2 %	2 %	2 %	2 %	2 %	2 %	2 %	2 %
Pulses	47													
– First season		21	1 %	1 %								1 %	1 %	1 %
– Second season		26			2 %	2 %	2 %	2 %	2 %					
Vegetables	205													
– First season		146	10 %	10 %	10 %	10 %								
– Second season		49					3 %	3 %	3 %	3 %				
– Third season		10									1 %	1 %	1 %	1 %
Citrus	78		5 %	5 %	5 %	5 %	5 %	5 %	5 %	5 %	5 %	5 %	5 %	5 %
Fruits	131		9 %	9 %	9 %	9 %	9 %	9 %	9 %	9 %	9 %	9 %	9 %	9 %
Oil crops	187		13 %	13 %	13 %	13 %	13 %	13 %	13 %	13 %	13 %	13 %	13 %	13 %
Sunflower	14				1 %	1 %	1 %	1 %	1 %					
Cotton	8				1 %	1 %	1 %	1 %	1 %	1 %	1 %			
Fodder (annual)	133		9 %	9 %	9 %							9 %	9 %	9 %
Fodder (perennial)	15		1 %	1 %	1 %	1 %	1 %	1 %	1 %	1 %	1 %	1 %	1 %	1 %
Sum over all crops	1465		81 %	81 %	93 %	77 %	46 %	46 %	46 %	39 %	31 %	71 %	71 %	72 %
Actually irrigated	1485													
Equipped for irrigation	1485													
Total cropping intensity	99 %													

outflow can be equal to the monthly inflow and F will be 1. Large sub-basins or sub-basins with high storage capacity have high retention times and therefore low values for the response factor F. For all sub-basins in this study a response factor F of 0.3 was assumed. No differentiation was made between different carry-over factors since analysing monthly differences in stream flow was beyond the scope of the study.

10 Irrigation efficiencies

GlobWat calculates the incremental evaporation over areas under irrigation. In the case of paddy rice, an additional volume of water is used for flooding to control weeds. This volume of water can be calculated by multiplying the area under irrigated paddy rice by a water layer of 20 cm. The total irrigation requirements can then be calculated as follows:

$$\mathrm{Irr}_{\mathrm{req}} = \left(E_{\text{incr-irr}}(\mathrm{yr}) \times A_{\mathrm{cell}} + 0.2 \times A_{\mathrm{paddy}}(\mathrm{yr})\right) \times 10, \quad (33)$$

with $\mathrm{Irr}_{\mathrm{req}}$ the total irrigation requirements per year (m^3), $E_{\text{incr-irr}}(\mathrm{yr})$ the incremental evaporation due to irrigation per year (mm), A_{cell} the area of the grid cell (ha) and $A_{\mathrm{paddy}}(\mathrm{yr})$ the harvested area under paddy irrigation per year (ha).

In order to calculate irrigation efficiencies, the total irrigation water requirements were compared with the amount of water withdrawn for irrigation as available in AQUASTAT (http://www.fao.org/nr/water/aquastat/data/query/index.html). Since the years for which AQUASTAT data on water withdrawals generally do not concur with the years for which the cropping calendars are derived, the most recent country values for agricultural water withdrawal were extrapolated towards the year for which cropping calendars are valid. This was done by using the item "Total area equipped for irrigation" as available in FAOSTAT (http://faostat.fao.org/site/377/default.aspx#ancor) in Eq. (34):

$$Q_{\mathrm{aww}}(\text{yr-cc}) = Q_{\mathrm{aww}}(\text{yr-aww}) \cdot \mathrm{AEI}(\text{yr-cc})/\mathrm{AEI}(\text{yr-aww}), \quad (34)$$

with Q_{aww} the agricultural water withdrawal per country ($m^3\,yr^{-1}$), AEI the total area equipped for irrigation per country (ha), yr-cc the year for which a cropping calendar is available, and yr-aww the year with the latest available country values for agricultural water withdrawal.

Table 3. Input data sets.

Map	Resolution	Source
Global maps of monthly precipitation	10 min	New et al. (2002)
Global maps of wet days per month	10 min	New et al. (2002)
Global maps of coefficient of variation of precipitation per month	10 min	New et al. (2002)
Global maps of monthly reference evaporation	10 min	Calculated according to FAO (Allen et al., 1998) with input data from New et al. (2002)
Maximum soil moisture storage capacity	5 min	Derived from the Harmonised World Soil Database, FAO (2012)
Maximum groundwater recharge flux	5 min	Derived from WHYMAP, BGR and UNESCO (2008)
Land use or vegetation type coefficient (*Kc*)	5 min	Derived from FAO's Global Agricultural Systems Map, FAO (2011b)
Global map of irrigation areas	5 min	Siebert et al. (2007)
Global map of lakes and wetlands	5 min	Derived from Lehner and Döll (2004)
Global map of river basins and sub-basins		FAO (2011b)

The average of the years for which cropping calendar data are available is 2004, and consequently the calculated outputs of GlobWat as presented here are on average valid for that year. Water withdrawal data in AQUASTAT that were estimated on the basis of earlier model calculations were excluded from the exercise.

Irrigation efficiencies can be calculated by applying Eq. (35) per country for those countries for which country data on agricultural water withdrawals are available. For those countries for which no water withdrawal data are available, irrigation efficiencies have been estimated based on countries nearby with similar conditions with regard to climate and economic development:

$$\mathrm{Irr_{eff}} = \mathrm{Irr_{req}}/Q_{\mathrm{aww}}, \quad (35)$$

with $\mathrm{Irr_{eff}}$ the irrigation efficiency (–), $\mathrm{Irr_{req}}$ the total irrigation requirements ($\mathrm{m^3\,yr^{-1}}$) and Q_{aww} the agricultural water withdrawal ($\mathrm{m^3\,yr^{-1}}$).

11 Input and output data sets

The input data sets used are derived from public domain data sets and are found in Table 3.

The results of the water balance calculations consist of monthly values by grid cell for generated precipitation, actual evaporation, incremental evaporation due to irrigated agriculture, surface runoff, groundwater recharge and water stored as soil moisture. Aggregated annual water balances can be calculated for any desired spatial domain (e.g. countries or river basins) and include, apart from the above-mentioned variables, incremental evaporation over open water and incremental evaporation over wetlands.

12 Model results, calibration and validation

Water balances have been generated by the model and aggregated for each country to compare them with AQUASTAT data on Internal Renewable Water Resources (IRWR) and "Internally produced groundwater". The internal renewable water resources of a country are defined as "Long-term average annual flow of rivers and recharge of aquifers generated from endogenous precipitation". It corresponds to the sum of surface runoff and groundwater recharge as calculated by the model. Internally produced groundwater is defined as "Long-term annual average groundwater recharge, generated from precipitation within the boundaries of the country", which was compared to the model-generated groundwater recharge (AQUASTAT datadase; FAO, 2013).

Calibration of the model was only undertaken for the "vertical" water balance (step 1 in Fig. 1). Calibration factors were applied for hydrologically more or less uniform AQUASTAT regions as described in "The state of the world's land and water resources for food and agriculture – Managing systems at risk" (FAO, 2011b). Two layers with calibration factors were used, one to adjust (sub-)surface runoff fluxes by multiplying the maximum soil moisture storage capacity, the effective rooting depth and the number of wet days by a calibration factor ($\mathrm{Cal_{sw}}$), and another one to fine-tune groundwater recharge by multiplying the maximum groundwater recharge flux by a groundwater calibration factor ($\mathrm{Cal_{gw}}$).

Table 4. Calibration factors per hydrological region.

Region	Cal-sw	IRWR (mm) AQUASTAT	Recharge and drainage (mm), modelled	Diff. (mm)	Cal-gw	Ground water recharge (mm) AQUASTAT	Ground water recharge (mm), modelled	Diff. (mm)
Northern Africa	1.5	9	8	0	1.5	3	2	0
Sudano–Sahel	2	19	38	20	1	7	6	−1
Gulf of Guinea	1.7	455	475	20	1.5	134	146	11
Central Africa	1.9	353	409	56	1.2	156	185	29
Eastern Africa	2	96	138	41	1.2	33	34	1
Southern Africa	2	57	101	44	1	17	24	7
Indian Ocean islands	1	571	590	20	1	94	109	15
North America	0.7	299	268	−31	2.5	92	84	−9
Mexico	1	210	206	−4	2.5	71	66	−5
Central America	0.7	1335	1306	−29	2.5	397	263	−134
Greater Antilles	0.9	440	389	−51	2.2	126	110	−15
Lesser Antilles	0.9	218	386	168	2.2	141	108	−33
Guyanas	0.9	1051	1109	58	2.5	512	333	−179
Andes	0.7	1106	1041	−64	2.5	278	194	−84
Brazil	1	638	761	123	2	221	311	91
South America	0.7	322	347	25	2.5	81	54	−27
Arabian Peninsula	2	2	7	4	2.5	2	0	−2
Caucasus	0.6	393	359	−34	2.5	151	72	−79
Iran	0.6	79	102	22	2.5	30	11	−20
Near East	0.7	181	163	−18	2.5	54	47	−7
Central Asia	0.7	57	73	16	2.5	9	22	13
South Asia	0.9	465	537	72	2.5	130	81	−49
East Asia	0.7	296	227	−69	2.5	77	57	−20
Mainland Southeast Asia	0.8	993	987	−5	2.5	326	200	−126
Maritime Southeast Asia	0.9	1323	1436	113	1	282	276	−6
Northern Europe	0.55	687	555	-133	2	120	112	−8
Western Europe	0.7	444	469	25	1	143	130	−13
Central Europe	0.75	228	223	−5	1	64	75	11
Mediterranean Europe	0.7	391	367	−24	2.4	89	97	9
Russian Federation	0.55	257	264	7	1.2	47	51	4
Eastern Europe	0.75	135	154	18	1	45	59	14
Australia and New Zealand	1	103	102	−1	1	9	11	1
Pacific Islands	0.7	1802	1779	−23	2	–	–	–

Cal_{sw} varies from 0.55 to 2 and Cal_{gw} from 1 to 2.5. The results of the calibration are presented in Table 4.

Validation of the model output was accomplished by comparing average river discharges of the Global River Discharge Database (Center for Sustainability and the Global Environment, 2014). The stations with discharge data in the Global River Discharge Database are not always located at the mouth of the river basin. Therefore the specific discharge, defined as the total annual discharge divided by the area over which the discharge is generated, was calculated for the stations situated as close as possible to the mouth of the river. The specific discharges per station were then compared with the specific discharge per river basin as derived from the modelled data. Table 5 shows the result of this validation exercise for 51 river basins with an area greater than 100 000 km^2. Figure 2 shows the same results in a graph.

The total area weighted average specific discharge as measured over the above-listed river basins is 332 mm per year. The area weighted average difference (observed minus simulated) in specific discharges is 2 mm, which indicates that the model underestimates the total discharge over all river basins by 0.7 %.

The model results have also been evaluated against the three quantitative statistical indicators recommended by Moriasi et al. (2007): the above-listed results have a Nash–Sutcliffe efficiency (NSE) of 0.90 (where 1 would be the ideal model), a percent bias (PBIAS) of −3.0 % (not taking into account the area of the basin, the model overestimates, on average per basin, the discharge by 3.0 %), and a root

Table 5. Validation results per river basin.

River basin	Measured			Modelled			Difference
	Discharge ($m^3 s^{-1}$)	Upstream area (km^2)	Specific discharge (mm)	Basin area (km^2)	Total outflow ($m^3 s^{-2}$)	Specific discharge (mm)	in specific discharge (mm)
Amazon	171 663	4 618 746	1172	5 987 204	209 190	1102	70
Congo	40 192	3 475 000	365	3 712 251	43 154	367	−2
Mississippi–Missouri	17 031	2 964 254	181	3 265 753	21 829	211	−30
Nile	2744	3 080 000	28	3 083 546	2733	28	0
Ob	12 475	2 430 000	162	3 010 822	13 422	141	21
Yenisey	17 682	2 440 000	229	2 561 252	19 465	240	−11
Lena	16 621	2 430 000	216	2 401 442	14 553	191	25
Niger	1149	1 000 000	36	2 142 881	7516	111	−74
Amur	9739	1 730 000	178	2 079 157	14 103	214	−36
Yangtze	25 031	1 705 383	463	1 791 327	23 602	416	47
Mackenzie	8343	1 570 000	168	1 755 147	2801	50	117
Ganges–Bramaputra	30 796	1 483 030	655	1 669 861	26 724	505	150
Volga	8086	1 360 000	188	1 466 717	12 280	264	−77
St Lawrence	6881	764 600	284	1 304 701	14 687	355	−71
Saskatchewan–Nelson	2402	1 000 000	76	1 131 261	607	17	59
Syr Darya	541	219 000	78	1 113 531	0	0	78
Orange	157	850 530	6	986 696	383	12	−6
Orinoco	28 723	850 000	1066	976 688	39 807	1285	−220
Murray–Darling	256	991 000	8	929 640	889	30	−22
Tocantins	12 173	758 000	506	916 945	21 781	749	−243
Tigris–Euphrates	1570	408 100	121	915 121	1336	46	75
Indus	2396	832 418	91	868 766	137	5	86
Huang He	1209	688 421	55	832 699	1671	63	−8
Mekong	7994	391 000	645	803 765	16 814	660	−15
Amu Darya	1500	450 000	105	798 035	0	0	105
Danube	6498	807 000	254	797 546	6770	268	−14
Colorado, North America	463	289 562	50	650 653	631	31	20
Sao Francisco	2817	510 800	174	638 834	2624	130	44
Rio Grande–Bravo	69	459 902	5	552 282	404	23	−18
Dnieper	1483	463 000	101	511 573	2214	137	−35
Senegal	665	218 000	96	478 482	882	58	38
Don	787	378 000	66	443 541	2678	190	−125
Xun Jiang	7084	329 705	678	412 937	9198	702	−25
Volta	1124	394 100	90	412 735	1971	151	−61
Limpopo	75	196 000	12	411 728	88	7	5
Colorado, South America	104	22 300	147	374 438	681	57	90
Parnaiba	842	282 000	94	332 770	1384	131	−37
Godavari	3061	299 320	323	314 617	4534	455	−132
Krishna	1641	251 355	206	274 596	1546	178	28
Northern Dvina	3315	348 000	300	273 375	3128	361	−60
Magdalena	6973	257 438	854	260 535	8646	1047	−192
Neva	2511	281 000	282	227 929	2471	342	−60
Wisla	1056	194 376	171	192 953	920	150	21
Rhine	2291	159 680	452	186 771	2361	399	54
Negro	762	95 000	253	161 660	990	193	60
Chao Phraya	776	110 569	221	157 633	1528	306	−84
Mahandi	1883	132 090	450	145 260	2893	628	−178
Elbe	744	123 532	190	140 390	883	198	−9
Grijalva–Usumacinta	2030	47 697	1342	132 063	4386	1047	295
Oder	536	109 729	154	120 587	567	148	6
Loire	835	110 000	239	116 573	1191	322	−83

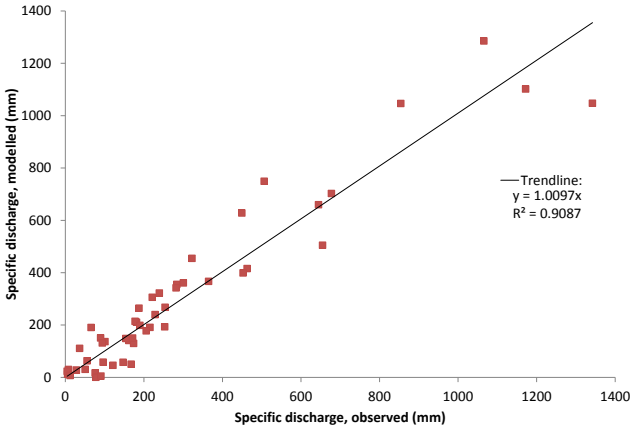

Figure 2. Graphic representation of validation results in which modelled specific river discharges are compared to observed specific river discharges.

mean square error–standard deviation ratio (RSR) of 0.31 (the RSR can vary from the optimal value of 0 – no residual variation, so perfect simulation – to a large positive value). According to Moriasi et al. (2007), model simulation can be judged as satisfactory if NSE > 0.50, PBIAS < ±25 %, and RSR < 0.70.

The outputs of the model are global raster maps with a resolution of 5 arcmin containing monthly information on generated precipitation, total actual evaporation from the soil water balance component, incremental evaporation from irrigation, incremental evaporation from lakes and wetlands, (sub-)surface runoff and groundwater recharge. The output maps are available on FAO's AQUAMAPS website: http://www.fao.org/nr/water/aquamaps/.

As an example, Fig. 3 shows total yearly actual evaporation (the sum of actual evaporation from the soil water balances and incremental evaporation from irrigated areas, lakes and wetlands).

Figure 4 shows the calculated accumulated outflow per sub-basin. Since the HydroSHEDS database does not provide data above 60° northern latitude, and due to the fact that in these areas population densities are generally low, the mapped sub-basins are of a lower spatial resolution, which can be seen in Greenland and the northern-flowing river basins in Siberia (e.g. Ob, Lena, Yenissey).

Apart from maps, the model also calculates aggregated results per country, per major basin and per sub-basin. As an example, the total global water balance as calculated by GlobWat is presented in Table 6.

In Table 7, incremental evaporation due to irrigation as calculated by GlobWat; total irrigation water requirements; amounts of water withdrawn for irrigation as available in AQUASTAT (http://www.fao.org/nr/water/aquastat/data/query/index.html); and irrigation efficiencies, are presented for the hydrological regions. Since more or less reliable water withdrawal data per country are available for less than 50 % of the countries included in this analysis, it was decided to present water use efficiency values for hydrological regions only rather than for individual countries.

Table 6. Global terrestrial water balance.

	10^9 m^3	(mm)
Precipitation	105 316	(805)
Rainfed evaporation	61 106	(467)
Renewable water resources	44 211	(338)
Incremental evaporation over open water	1184	(9)
Incremental evaporation over wetlands	2899	(22)
Incremental evaporation from irrigation	1268	(10)
Outflow to sea	38 859	(297)

Figure 5 shows the distribution of global water stress by major river basin based on incremental evaporation caused by irrigation as a percentage of total generated groundwater and surface water resources. Levels of water stress are often classified by using the Millennium Development Goals – Water Indicator. The MDG Water Indicator measures water stress per country on the ratio between total water withdrawn and total renewable water resources (UN, 2008; FAO, 2013). Using this indicator, it is estimated that a withdrawal rate above 20 % of renewable water resources represents "substantial" pressure on water resources, while more than 40 % is considered "critical" (FAO 2011b). Other classifications use thresholds of 0–10 % no stress, 10–20 %, low stress, 20–40 % moderate stress, and more than 40 % severe stress (UN, 1997). The mentioned stress classifications include all water withdrawals. Taking into account that agriculture accounts for more than 90 % of the consumptive use of global water withdrawals (FAO, 2012), and that on average incremental evaporation due to irrigation is about half of irrigation water withdrawals (Table 8), it is possible to assume thresholds of water stress classes based on incremental evaporation that are half of the thresholds based on water withdrawals. Water stress can then be considered substantial when incremental evaporation caused by irrigation exceeds 10 % of the generated water resources in a river basin. River basins in which the incremental evaporation caused by irrigation exceeds 20 % should be considered critically stressed.

13 Discussion and conclusion

Modelling exercises, performed with earlier versions of the model and with other input data sets, have been used by FAO on several occasions and were documented in the following FAO perspective studies: World agriculture: towards 2015–30; an FAO perspective (Bruinsma, 2003), World Agriculture – Towards 2030 and 2050 (FAO, 2006), World Agriculture – Towards 2050 and 2080 (FAO, 2011a), and the global assessment of water use and availability carried out for The State of the World's Land and Water Resources for Food and Agri-

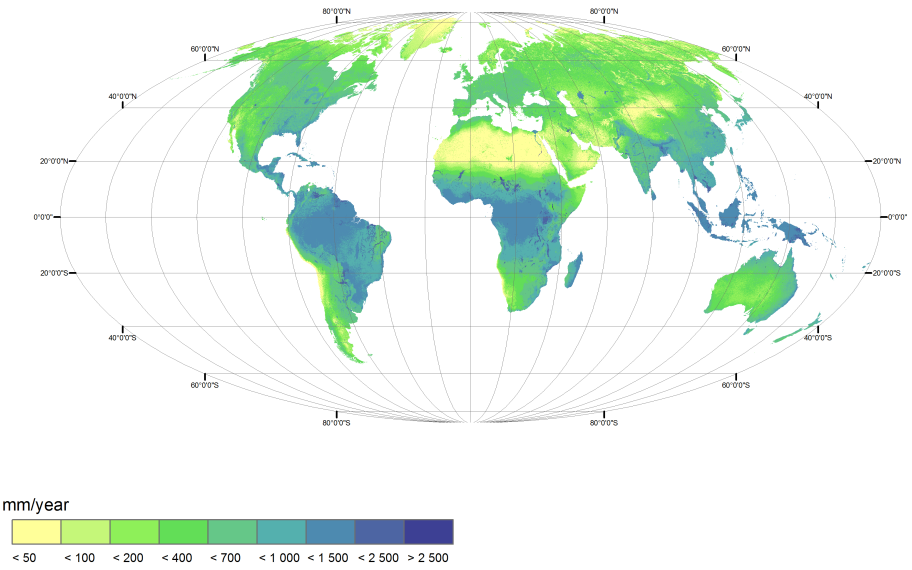

Figure 3. Average global actual evaporation per year.

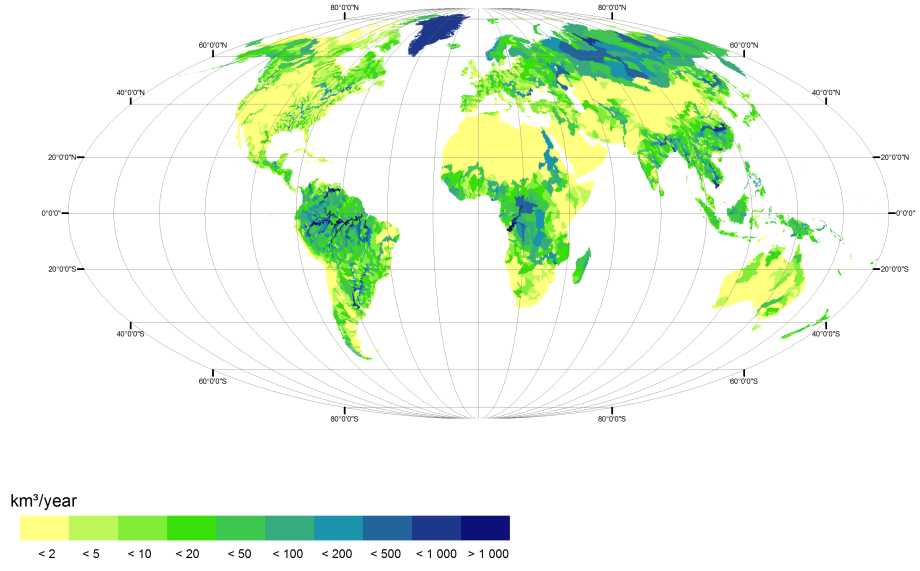

Figure 4. Average annual outflow per sub-basin.

culture (FAO, 2011b). However, the model results were never systematically compared with the outputs of other models. For this article, the output of GlobWat is compared with models WaterGAP, WBMplus, GEPIC, LPJmL, PCR-GLOBWB and GCWM as mentioned in the introduction of this article. In Table 8 the calculated amount of water used in agriculture for these models is compared with the results of GlobWat. Values for the incremental evaporation due to irrigation for all models except PCR-GLOBWB were found in Hoff et al. (2010). Values for the incremental evaporation due to irrigation PCR-GLOBWB, and values on water withdrawal for irrigation, were found in the references mentioned above.

Table 8 shows that the values of "incremental evaporation due to irrigation" are fairly similar among the different models (except for GEPIC, which shows significantly lower results than the other models). With regard to the "water withdrawals for irrigation", the results of GlobWat and LPJmL are very similar, and, to a lesser extent, so are the results from WaterGap2 and WBMplus. This implies that the irrigation efficiencies as assumed by WaterGAP2 and WBMplus (around 38 %) are significantly lower than those from GlobWat and LPJmL (around 50 %). Irrigation efficiencies for PCR-GLOBWB are in between these values at around 41 %. The calculated irrigation efficiency for GlobWat (55 %) is higher than the irrigation efficiencies for all other models.

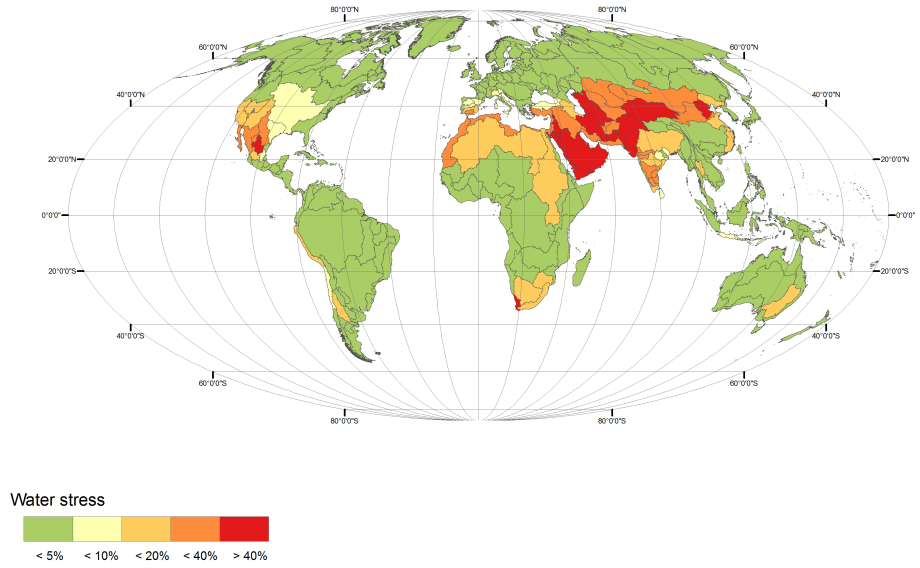

Figure 5. Water stress per major river basin expressed as a percentage of incremental evaporation due to irrigation over generated groundwater and surface water resources.

This is mainly due to the fact that for GlobWat also the water requirements for flooding paddy rice are incorporated into the irrigation water requirements. If the irrigation efficiency of GlobWat would be calculated as incremental evaporation divided by water withdrawals, it would result in a value of 48 %.

In addition to the higher resolution as compared to most other global (agro)hydrological models, GlobWat differs from these models in the explicit differentiation between evaporation from in situ rainfall and incremental evaporation occurring over wetlands, open water and irrigated areas of water that is conveyed from elsewhere. This distinction is especially useful for differentiating between the part of the evaporation that can be influenced only through land management (evaporation from in situ rainfall or "green water") and the part of the evaporation that is influenced through water management (incremental evaporation or "blue water").

For "open water" and "swamps and wetlands" GlobWat makes, unlike other models, a clear distinction between the "vertical" water balance, attributable to in situ rainfall, and the "horizontal" balance, attributable to lateral flow. This distinction is not only important in terms of the internal consistency of the model concept over all land cover classes, it is especially relevant for the calculation of renewable water resources. In the model, renewable water resources are calculated as the sum of all generated groundwater and surface water, which equals precipitation minus evaporation from in situ precipitation. If the precipitation exceeds evaporation, the precipitation surplus over open water and wetlands contributes to the renewable water resources. However, if evaporation exceeds precipitation over open water and wetlands, (the evaporation "surplus"), the incremental evaporation over open water and wetlands is not incorporated into the calculation of generated renewable water resources. This is necessary to account for water resources generated in internal river basins, which would otherwise be classified as having no renewable water resources at all.

Excluding the incremental evaporation over wetlands and open water has as a consequence that some river basins in Fig. 5 (e.g. the Nile River basin) seem to be less stressed than is apparent. In the case of the Nile basin, the lower than expected stress levels are due to water losses over wetlands and open water. According to the GlobWat results, more than 50 % of all the water resources that are generated in the Nile River basin evaporate as incremental evaporation over open water and wetlands, specifically over the Sudd wetlands.

In conclusion, GlobWat is a simple model that has been designed specifically to assess the impact of irrigated agriculture on the global hydrological cycle. The model was calibrated using country-level data on total internal renewable water resources and groundwater resources, and validated with discharge data from major river basins. The model has a high resolution of 5 min and distinguishes between evaporation from in situ rainfall and from water transported in from elsewhere. Model outputs include estimates of consumptive water use by agriculture which were compared with AQUASTAT country data on water withdrawals for agriculture to calculate irrigation efficiencies.

GlobWat, including all input data sets, will be made freely available for download at FAO's AquaMaps website: http://www.fao.org/nr/water/aquamaps/.

Table 7. Water use in agriculture per hydrological region.

Region	Incremental evaporation due to irrigation (10^6 m^3)	Total irrigation requirements (10^6 m^3)	Irrigation "efficiency"*	Irrigation water withdrawals (10^6 m^3)
Northern Africa	55 975	57 291	69 %	83 388
Sudano–Sahel	11 019	11 608	42 %	27 825
Gulf of Guinea	2077	2203	43 %	5183
Central Africa	241	272	24 %	1151
Eastern Africa	2773	3033	25 %	12 294
Southern Africa	8730	8767	41 %	21 283
Indian Ocean islands	2273	4398	21 %	21 220
North America	108 903	111 072	56 %	199 842
Mexico	25 902	26 034	43 %	61 200
Central America	3726	3920	48 %	8246
Greater Antilles	1863	2348	38 %	6181
Lesser Antilles	56	104	38 %	274
Guyanas	346	711	36 %	1992
Andes	16 912	18 225	31 %	58 129
Brazil	13 038	15 296	48 %	31 700
South America	18 452	19 303	51 %	37 570
Arabian Peninsula	20 936	20 936	57 %	36 741
Caucasus	4492	4492	37 %	12 224
Iran	47 929	49 185	55 %	88 844
Near East	49 854	50 092	51 %	98 361
Central Asia	59 853	60 621	47 %	127 883
South Asia	469 665	531 646	58 %	909 744
East Asia	205 531	269 871	71 %	382 570
Mainland Southeast Asia	47 670	79 094	46 %	173 709
Maritime Southeast Asia	30 242	57 469	39 %	148 697
Northern Europe	813	813	58 %	1397
Western Europe	4497	4497	72 %	6282
Central Europe	1107	1115	42 %	2668
Mediterranean Europe	29 552	30 358	69 %	43 765
Russian Federation	8949	9227	42 %	22071
Eastern Europe	2300	2342	42 %	5602
Australia and New Zealand	12 051	12 089	64 %	18 787
Pacific Islands	0	0	–	0
World	1 267 727	1 468 433	55 %	2 656 825

* Calculated according to Eq. (35).

Table 8. Global water use in agriculture as calculated by different models.

Model	Water withdrawals for irrigation (km^3 yr^{-1})	Total irrigation requirements (km^3 yr^{-1})	Incremental evaporation due to irrigation (km^3 yr^{-1})	Reference year	Spatial resolution	Irrigation efficiency
GlobWat	2657	1468	1268	On average, 2004	5 arcmin	55 %
WaterGAP2	3594	–	1300	1995	30 arcmin	36 %
WBMplus	3250	–	1301	1998–2002	30 arcmin	40 %
LPJmL	2650	–	1364	1981–2000	30 arcmin	51 %
GEPIC	–	–	927	2000	30 arcmin	–
GCWM	–	–	1180	1998–2000	5 arcmin	–
PCR-GLOBWB (CRU TS2.1 – ref. scen.)	2885	–	1179	2000	30 arcmin	41 %

Edited by: J. Liu

References

Alcamo, J., Flörke, M., and Märker, M.: Future long-term changes in global water resources driven by socio-economic and climatic changes, Hydrolog. Sci. J., 52, 247–275, 2007.

Allen, R. G., Pereira, L. S., Raes, D., and Smith, M.: Crop evapotranspiration, Guidelines for computing crop water requirements, Irrigation and Drainage Paper 56, Food and Agriculture Organization of the United Nations, Rome, Italy, 1998.

BGR and UNESCO: World-wide Hydrogeological Mapping and Assessment Programme (WHYMAP), Hannover, Germany, 2008.

Biemans, H.: Water constraints on future food production, Wageningen University dissertation no. 5319, Wageningen, the Netherlands, 2012.

Bruinsma, J. (Ed.): World agriculture: towards 2015/2030, An FAO perspective, Earthscan, London, UK and Food and Agriculture Organization of the United Nations, Rome, Italy, 2003.

Center for Sustainability and the Global Environment (SAGE): Global River Discharge Database, http://www.sage.wisc.edu/riverdata/, last access: 12 March 2014.

De Zeeuw, J. W.: Hydrograph analysis for areas with mainly groundwater runoff, in: Drainage Principle and Applications, Vol. II, Chapter 16, Theories of field drainage and watershed runoff, Publication 16, International Institute for Land Reclamation and Improvement (ILRI), Wageningen, The Netherlands, 321–358, 1973.

Döll, P. and Fiedler, K.: Global-scale modeling of groundwater recharge, Hydrol. Earth Syst. Sci., 12, 863–885, doi:10.5194/hess-12-863-2008, 2008.

Evans, R., Cassel, D. K., and Sneed, R. E.: Soil, water, and crop characteristics important to irrigation scheduling, Publication No. AG 452-1, North Carolina Cooperative Extension Service, Raleigh, North Carolina, 1996.

Falkenmark, M. and Rockström, J.: Balancing Water for Humans and Nature, The New Approach in Ecohydrology, Earthscan, London, UK, 247 pp., 2004.

FAO: Effective rainfall in irrigated agriculture, Food and Agriculture Organization of the United Nations, Rome, Italy, 1978.

FAO: World agriculture: towards 2030/2050, Interim report, Food and Agriculture Organization of the United Nations, Rome, Italy, 2006.

FAO: World agriculture: towards 2050/2080, Food and Agriculture Organization of the United Nations, Rome, Italy, 2011a.

FAO: State of the world's land and water resources for food and agriculture (SOLAW), Managing systems at risk, Food and Agriculture Organization of the United Nations, Rome, Italy and Earthscan, London, UK, 2011b.

FAO: Coping with water scarcity – An action framework for agriculture and food security, Food and Agriculture Organization of the United Nations, Rome, Italy, 2012.

FAO: AQUASTAT database, Food and Agriculture Organization of the United Nations, Rome, Italy, http://www.fao.org/nr/water/aquastat/main/index.stm (last access: 12 March 2015), 2013.

FAO/IIASA: Global Agro-Ecological Zones database, Food and Agriculture Organization of the United Nations, Rome, Italy and IIASA, Laxenburg, Austria, http://gaez.fao.org/Main.html (last access: 30 November 2014), 2012.

FAO/IIASA/ISRIC/ISSCAS/JRC: Harmonized World Soil Database (version 1.2), Food and Agriculture Organization of the United Nations, Rome, Italy and IIASA, Laxenburg, Austria, 2012.

Hoekstra, A. Y. and Chapagain, A. K.: Water footprints of nations: Water use by people as a function of their consumption pattern, Water Resour. Manage., 21, 35–48, 2007.

Hoff, H., Falkenmark, M., Gerten, D., Gordon, L., Karlberg, L., and Rockström, J.: Greening the global water system, J. Hydrol., 384, 177–186, 2010.

Hunger, M. and Döll, P.: Value of river discharge data for global-scale hydrological modeling, Hydrol. Earth Syst. Sci., 12, 841–861, doi:10.5194/hess-12-841-2008, 2008.

Lehner, B. and Döll, P.: Development and validation of a global database of lakes, reservoirs and wetlands, J. Hydrol., 296, 1–22, 2004.

Liu, J.: A GIS-based tool for modelling large-scale crop-water relations, Environ. Modell. Softw., 24, 411–422, 2009.

Liu, J. and Yang, H.: Spatially explicit assessment of global consumptive water uses in cropland: Green and blue water, J. Hydrol., 384, 187–197, 2010.

Moriasi, D. N., Arnold, J. G., Van Liew, M. W., Bingner, R. L., Harmel, R. D., and Veith, T. L.: Model evaluation guidelines for systematic quanti?cation of accuracy in watershed simulations, Trans. ASABE, 50, 885–900, 2007.

New, M., Lister, D., Hulme, M., and Makin, I.: A high-resolution data set of surface climate over global land areas, Clim. Res., 21, 1–25, 2002.

Portmann, F., Siebert, S., Bauer, C., and Döll, P.: Global data set of monthly growing areas of 26 irrigated crops, Frankfurt Hydrology Paper 06, Institute of Physical Geography, University of Frankfurt, Frankfurt am Main, Germany, 2008.

Raes, D., Steduto, P., Hsiao, T. C., and Fereres, E.: Reference Manual AquaCrop Version 4.0, Food and Agriculture Organization of the United Nations, Rome, Italy, 2012

Rost, S., Gerten, D., Bondeau, A., Lucht, W., Rohwer, J., and Schaphoff, S.: Agricultural green and blue water consumption and its influence on the global water system, Water Resour. Res., 44, W09405, doi:10.1029/2007WR006331, 2008.

Savenije, H. H. G.: The importance of interception and why we should delete the term evapotranspiration from our vocabulary, Hydrol. Process., 18, 1507–1511, 2004.

Schoof, J. T. and Pryor, S. C.: On the Proper Order of Markov Chain Model for Daily Precipitation Occurrence in the Contiguous United States, J. Appl. Meteorol. Clim., 47, 2477–2486, 2008.

Siebert, S. and Döll, P.: The Global Crop Water Model (GCWM): Documentation and first results for irrigated crops, Frankfurt Hydrology Paper 07, Institute of Physical Geography, University of Frankfurt, Frankfurt am Main, Germany, 2008.

Siebert, S. and Döll, P.: Quantifying blue and green virtual water contents in global crop production as well as potential production losses without irrigation, J. Hydrol., 384, 198–217, 2010.

Siebert, S., Döll, P., Feick, S., Hoogeveen, J., and Frenken K.: Global Map of Irrigation Areas version 4.0.1, Johann Wolfgang Goethe University, Frankfurt am Main, Germany and Food

and Agriculture Organization of the United Nations, Rome, Italy, 2007.

Siebert, S., Burke, J., Faures, J. M., Frenken, K., Hoogeveen, J., Döll, P., and Portmann, F. T.: Groundwater use for irrigation – a global inventory, Hydrol. Earth Syst. Sci., 14, 1863–1880, doi:10.5194/hess-14-1863-2010, 2010.

Siebert, S., Henrich, V., Frenken, K., and Burke, J.: Update of the digital global map of irrigation areas to version 5, Rheinische Friedrich-Wilhelms-Universität, Bonn, Germany and Food and Agriculture Organization of the United Nations, Rome, Italy, 2013.

Steenhuis, T. S. and van der Molen, W. H.: The Thornthwaite-Mather Procedure as a Simple Engineering Method to Predict Recharge, J. Hydrol., 84, 221–229, 1986.

UN: Comprehensive assessment of the freshwater resources of the world – Report of the Secretary-General, United Nations Department of Economic and Social Affairs, New York, 1997.

UN: Official list of MDG indicators, United Nations, New York, 2008.

Wada, Y., Wisser, D., and Bierkens, M. F. P.: Global modeling of withdrawal, allocation and consumptive use of surface water and groundwater resources, Earth Syst. Dynam., 5, 15–40, doi:10.5194/esd-5-15-2014, 2014.

Wilks, D. S. and Wilby, R. L.: The weather generation game: a review of stochastic weather models, Prog. Phys. Geogr., 23, 329–357, 1999.

Wisser, D., Frolking, S., Douglas, M. E., Fekete, B. M., Schumann, A. H., and Vörösmarty, C. J.: Blue and green water: The significance of local water resources captured in small reservoirs for crop production – a global scale analysis, J. Hydrol., 384, 264–275, 2010.

Wood, E. F., Roundy, J. K., Troy, T. J., van Beek, L. P. H., Bierkens, M. F. P., Blyth, E., de Roo, A., Döll, P., Ek, M., Famiglietti, J., Gochis, D., van de Giesen, N., Houser, P., Jaffé, P. R., Kollet, S., Lehner, B., Lettenmaier, D. P., Peters-Lidard, C., Sivapalan, M., Sheffield, J., Wade, A., and Whitehead P.: Hyperresolution global land surface modeling: Meeting a grand challenge for monitoring Earth's terrestrial water, Water Resour. Res., 47, W05301, doi:10.1029/2010WR010090, 2011.